

WIDEBAND WIRELESS PROPAGATION IN CONFINED SPACES

Asrar U. H. Sheikh, M. Imran Akram and Khurram Masood

Electrical Engineering Department, King Fahd University of Petroleum and Minerals, 31261 Dhahran, Saudi Arabia

Keywords: Radio propagation, Indoors, Impulse response, Modeling.

Abstract: This paper presents the results of channel sounding experiment performed in confined environment. The swept time-delay cross-correlation technique is used as a method for sounding to measure the channel impulse response (CIR). PDF of the envelope and power for the received CIR is presented. The path loss exponent has been calculated. The data has been analysed for impulse response and channel parameters like average delay, rms delay spread, number of paths and channel bandwidth. The CIR is used in calculation of total received power.

1 INTRODUCTION

Wireless and personal communication networks (WPCN) operating in the frequency range upto 3 GHz proposed for wireless communications in confined spaces have significant advantages over wired telephone networks. Random distributions of reflectors, scatterers and people movement make the confined channel time variant. This makes the radio propagation inside such environment a complex phenomenon. Thus, to design an efficient wireless network, it is deemed essential to understand the nature of channel in the confined spaces. Many researchers have studied the indoor radio propagation in 900 MHz and 1 to 2 GHz frequency bands and provided information on channel parameters (Seidel and Rappaport, 1992), (Hawbaker and T.S.Rappaport, 1990), (U. Dersch and Zollinger, 1994). (A. Chandra, 1999) investigates distance dependence propagation of radio waves at 450 MHz, 900 MHz, 1.35 GHz and 1.89 GHz in the corridor of the second, first and ground floor of an institute building. Measurement and characterization of multiple antenna system has been performed in (Poon and Ho, 2003). Reference (X. Zhao, 2002) deals with the outdoor measurement data at 5.3 GHz. The measurements were performed in urban, suburban and rural environments. (SALOUS, 1999) deals with the both indoor and outdoor measurements and characterization using chirp sounder.

Path loss in an indoor environment is very severe most of the time. It is also very dynamic, changing appreciably over short distances. Simple path loss rules are successful in describing the mobile channel, but not the indoor channel (Asrar Sheikh,

2010). The channels parameters have great dependence on the shape, size and construction of the building (H.Hashemi, 1993).

Researchers have studied the radio propagation in confined spaces in UWB frequency bands (Simon Chiu and Michelson, 2010), (Abdellah Chehri,) for making available information on channel parameters. Due to increase in voice and data traffic, the channel characterization of confined environment has become important. For this purpose, this paper focuses on the channel characterization in confined spaces. Experiments have been conducted and data has been analyzed to determine key parameters for such environments. These include the path loss exponent, path arrival time, excess delay, delay spread, bandwidth and the diffraction loss.

The paper has been arranged in the following order. Section 2 presents the details of channel sounding system used. In Section 3 the details of the experiments along with the analysis and results are presented. Finally Section 4 concludes the paper.

2 CHANNEL SOUNDING SYSTEM

Channel sounders were first used for mobile radio sounding by Young and Lacy at 450 MHz (Young W. R., 1950) in urban New York City with a pulse duration of 500 ns and later by Turin (Turin G. L., 1972). De Lange (E., 1952) also used 3 ns pulses for propagation studies at 4 GHz. The channel sounder used here overcomes the limitations of old sounder. It

utilizes the swept time-delay cross-correlation technique which is a very well known method of channel sounding. A pseudo-random bit sequence (PRBS) of length 511 and a chip rate of 30 MHz is used to phase reversal modulate an RF carrier signal at 1.8 GHz which is amplified and then transmitted. At the receiver, the incoming signal is correlated with a local oscillator signal which is phase-reversal modulated by a pseudo-random binary sequence identical to that at the transmitter but clocked at a slightly slower rate. The output of the correlation process represents the impulse response of the multipath channel, scaled in time. The normalized auto-correlation function $R_c(t)$, for a maximum length pseudo-random binary sequence (PRBS) of length N is given by the following relation:

$$R_c(t) = \begin{cases} 1 + \frac{1+(\frac{1}{N})t}{\tau_0}, & \text{for } -\tau_0 \leq t \leq 0 \\ 1 - \frac{1+(\frac{1}{N})t}{\tau_0}, & \text{for } 0 \leq t \leq \tau_0 \\ -\frac{1}{N}, & \text{otherwise} \end{cases} \quad (1)$$

where τ_c is the chip duration which equals to 33 nsec in our case. It is easy to see that each echo will have a base width of $2\tau_c$. To record one sample per delay bin at a chip rate of 30 MHz, the sampling rate is given by:

$$\text{sampling rate} = \frac{1 \text{ sample}}{\text{chip duration} \times \text{scaling factor}} \quad (2)$$

The output of the correlation process is equivalent to the time scaled version of the impulse response of the channel. The scaling factor is determined by the ratio of transmitter chip rate and slip rate (the difference in clock rate) and is given by:

$$\text{sampling factor} = \frac{\text{chip rate}}{\text{slip rate}} \quad (3)$$

For two samples per delay bin will require a sampling rate of 16 Hz and for 4 samples per delay bin the sampling rate is doubled to 32 KHz. In our case the sliding correlator uses a 30 MHz chip rate and 8 KHz slip rate to give a time scaling and bandwidth compression factor of 3750. Thus, for a sequence length of 511 and sampling rate of 28 KHz, the power delay profile length 17.1 μ sec is recorded in 64.125 msec after time scaling.

2.1 System Calibration

Calibration of the measurement system is important. For this purpose we use back to back tests with different known attenuations. The receiver video output is in the form of voltage. This means the voltage that is received in the range from 0 - 10 V is converted

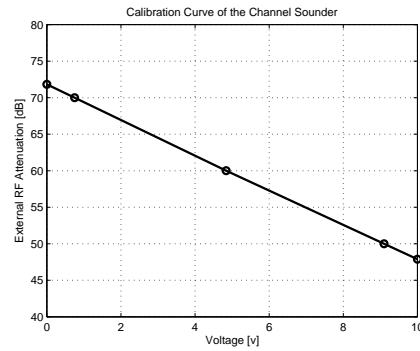


Figure 1: Calibration curve of the channel sounder system.

to power in dB using the calibration equation derived. For the back to back tests the transmitter was connected to the receiver via an external RF attenuator having a wide range of adjustment. The tests were performed by adjusting the setting of the attenuator in the range from 50 to 70 dB. The corresponding received voltages were used in obtaining the following attenuation equation

$$P_t(\text{dB}) = -2.4V + 71.7 - \text{AGC} \quad (4)$$

where AGC is the automatic gain control used at the receiver side to avoid the clipping of received signal. The corresponding calibration curve is shown in Figure 1. The absolute received power is calculated using following relations

$$P_r(\text{dBm}) = P_t(\text{dBm}) - P_l(\text{dB}) \quad (5)$$

where P_t and P_r are the transmitted and received power respectively and P_l is the corresponding attenuation. For the channel sounder used in experimentation the transmitted power is fixed at 10 dBm.

3 EXPERIMENTAL DATA AND ANALYSIS

3.1 Experimental Setup

The data was collected in the car park (B3) and corridors of Lab (LA), Ground (G) and 1st floor in Electrical Engineering Department building at KFUPM. Measurements are taken at regular intervals along the LOS path and also along the path perpendicular to the LOS corridor in order to calculate the path loss exponent and diffraction loss as shown in Figure 2 to Figure 4.

3.2 Data Analysis

The pdf of the envelop and power of 1st path for all the confined spaces is given in Figure 5 to 8. Ta-

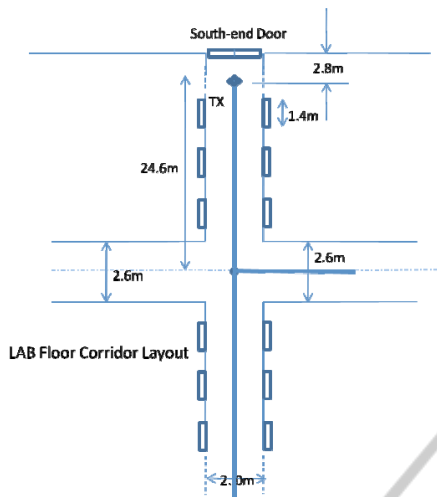


Figure 2: Layout for LA floor.

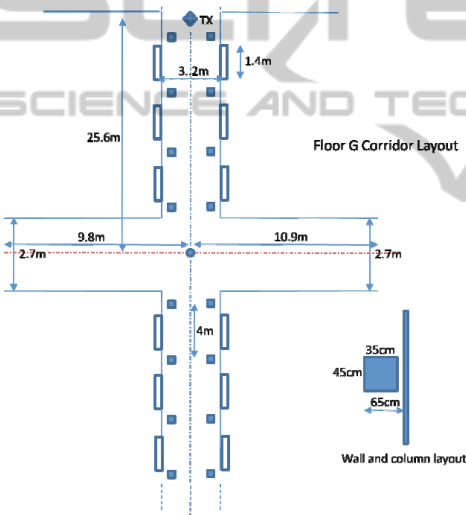


Figure 3: Layout for Ground floor.

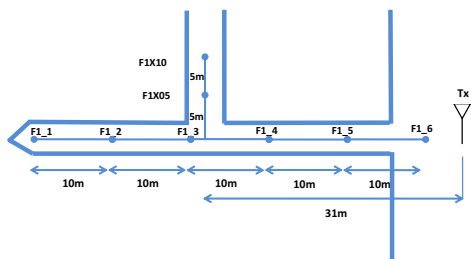


Figure 4: Layout for 1st floor.

Table 1 gives the arrival time statistics for the confined spaces. Arrival time for 3 paths has been listed for Car park B3, Floor LA and Ground Floor whereas for Floor 1 there are only 2 path arrival times which are listed. Floor G has a large arrival time for the 2nd and 3rd path, which is due to the NLOS data. Also

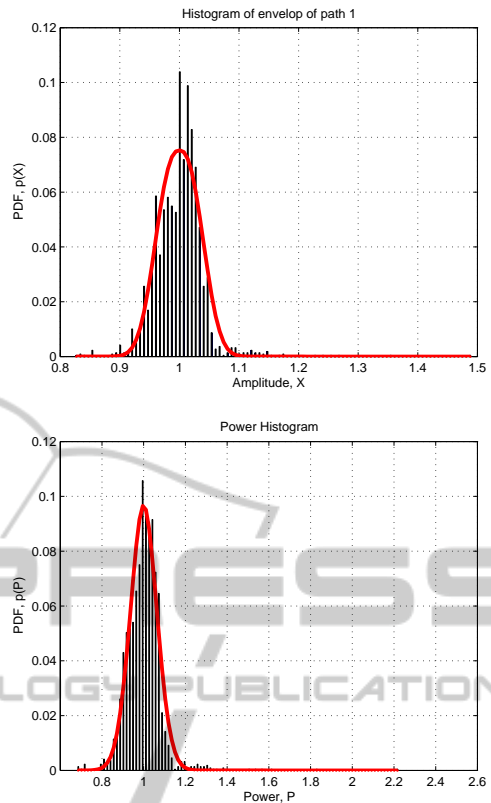


Figure 5: Amplitude and power PDF for B3.

for the Floor 1 we have a large arrival time for the 2nd path, which is due to the presence of open space when the data is recorded (Asrar Sheikh, 2010). Table 2 gives the received power as the sum of all the peaks in the CIR for the car park B3. The distances

Table 1: Path arrival time for different confined spaces.

	1 st path [nsec]	2 nd path [nsec]	3 rd path [nsec]
Car park B3	39.9064	92.1170	144.3275
Floor LA	31.1987	89.5895	141.7143
Floor Ground	30.858	198.62	775
Floor 1	26.5	168.6	—

between the transmitter and receiver are also given for different observations. Similar readings are given for other confined spaces in Table 3, 4 and 5. The calculations for the path loss exponent for these confined spaces gives us the values as shown in Table 6. As can be seen from the Figure 4, there is an opening in the corridor at 31 meters from the transmitter. This results in two different scenarios and hence the 2 path loss exponents as given in Table 6. Table 7 summarizes the measured channel parameters - number of paths, average access delay, rms delay spread and the coherence bandwidth. It should be noted that

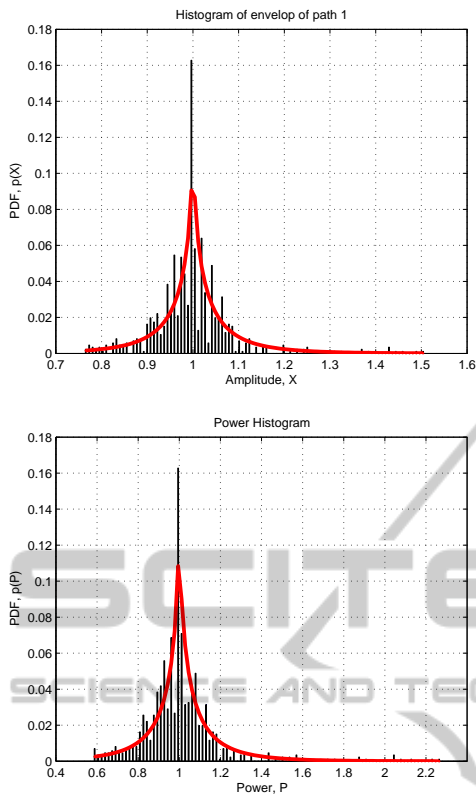


Figure 6: Amplitude and power PDF for LA.

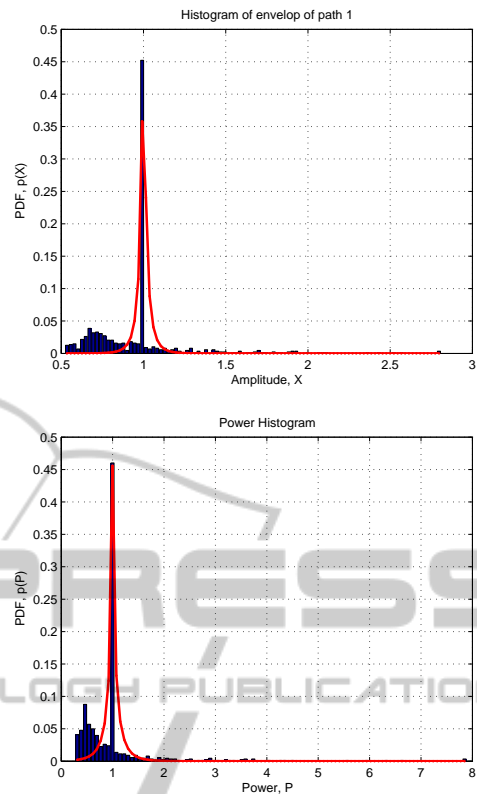


Figure 7: Amplitude and power PDF for FG.

Table 2: Car park (B3) Tx and Rx distances and received power.

Name	Dist. [m]	Power [dBm]	Name	Dist. [m]	Power [dBm]
B3_1	10	-24.83	B3_8	80	-42.22
B3_2	20	-27.34	B3_9	90	-35.29
B3_3	30	-26.00	B3_10	110	-33.25
B3_4	40	-26.40	B3_11	120	-34.97
B3_5	50	-34.17	B3_12	130	-38.03
B3_6	60	-42.71	B3_13	140	-41.29
B3_7	70	-44.08	B3_14	150	-38.02

Table 3: Floor LA Tx and Rx distances and received power.

No.	Name	Distance [meters]		Power [dBm]
		LOS	Lateral	
1	LA_1	16	0	-37.05
2	LA_2	18	0	-37.51
3	LA_3	25	0	-36.99
4	LA_4	25	8	-47.14
5	LA_5	16.5	5	-46.12

the maximum number of paths has been limited to 10 for the analysis. This is visible in the paths column for Floor LA, where 10 paths are listed. Also the data with single path received is not included in the table.

Diffraction loss is defined as that part of the re-

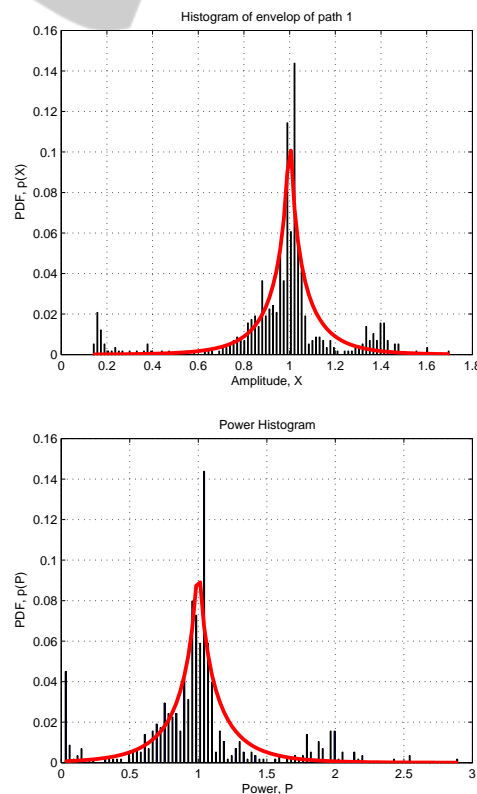


Figure 8: Amplitude and power PDF for F1.

Table 4: Ground Floor Tx and Rx distances and received power.

No.	Name	Distance [meters]		Power [dBm]
		LOS	Lateral	
1	FG_1	23	0	-37.04
2	FG_2	25.5	4.5	-38.10
3	FG_3	25.5	6.5	-39.86
4	FG_4	25.5	9.5	-44.53
5	FG_5	25.5	11	-39.46

Table 5: Floor 1 Tx and Rx distances and received power.

No.	Name	Distance [meters]	Power [dBm]
1	F1_1	54	-32.23
2	F1_2	44	-27.65
3	F1_3	34	-21.9
4	F1_4	24	-28.08
5	F1_5	14	-23.89
6	F1_6	04	-13.28

Table 6: Path loss exponent.

No.	Confined Space	Path loss Exponent n
1	Car park B3	1.21
2	Lab Floor LA	2.06
3	Ground Floor FG	0.91
4	1 st Floor F1	1.93 and 5.14

duction in power of a propagating wave or beam that results from diffraction. The diffraction loss has been calculated for Floor 1 with lateral distances of 5 and 10 meters. The calculated distances and power values are tabulated in Table 8. The received power at 31.98 and 33.88 meters from the transmitter are calculated by interpolation. The Diffraction loss can be approximated using the Knife Edge diffraction model given in (T.S.Rappaport, 2002).

$$P_{dl}(dB) = 13 + 20\log(v) \quad (6)$$

where

$$v = h\sqrt{\frac{2}{\lambda}\left(\frac{1}{D_T} + \frac{1}{D_R}\right)} \quad (7)$$

Where P_{dl} is the diffraction loss, v is the Fresnel parameter, λ is the wavelength (16.7 cm) corresponding to 1.8 GHz frequency. Here h , D_T and D_R are the height, transmitter and receiver distances respectively as shown in the Figure 9. From this, The value of v and P_{dl} are obtained as given in Table 8. The table shows that the measured and calculated values are comparable. Similar approach has also been used previously by (J. Francois, 1990) which shows the validity of this model where it has been mentioned that on the same floor the vertical polarization has an advantage of 4 dB over horizontal polarization.

Table 7: Summary of channel parameters for Confined Spaces.

Data File Name	Paths	Average Excess Delay μsec	RMS Delay Spread μsec	B_c kHz
B3_20	2	0.0057	0.0482	4147.8
B3_30	2	0.0041	0.0400	5005.4
B3_60	2	0.0120	0.0547	3654.0
B3_70	3	0.0144	0.0507	3948.6
B3_80	2	0.0057	0.0394	5076.0
B3_9	2	0.0105	0.0437	4579.7
B3_11	2	0.0021	0.0314	6375.9
LA_1	10	0.0290	0.1641	1218.9
LA_2	10	0.0508	0.3269	611.8
LA_3	10	0.0318	0.1644	1216.4
LA_4	10	0.1028	0.1413	1415.3
LA_5	10	0.0857	0.1511	1323.3
FG_1	4	3.9195	2.4601	81.3
FG_2	9	1.1377	0.6028	331.8
FG_3	7	0.5840	0.6551	305.3
FG_4	9	1.2416	1.0256	195.0
FG_5	8	1.5303	1.1179	178.9
F1_5	2	0.0025	0.0301	6650.5
F1_6	2	0.0103	0.0436	4582.4

Table 8: Diffraction Loss.

Lat. Dist [m]	D_T [m]	D_R [m]	h [m]	Fres. Para. v	Diff. Loss P_{dl}	
					Calc. [dB]	Meas. [dB]
5	30.62	1.36	4.91	14.92	36.5	30.1
10	29.7	4.18	9.13	16.51	37.4	31.1

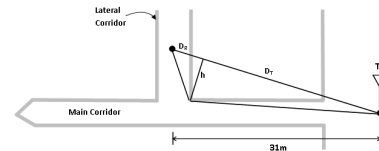


Figure 9: Diffraction Loss Knife edge model.

4 CONCLUSIONS

Channel sounding experiment conducted in confined environment has been presented in this paper. The path loss for the LOS has been computed using the sum of power of all the paths received. Path loss exponent for Floor LA and Floor 1 is closer to 2 (for free space), suggesting a line of sight (LOS) propagation in these spaces. The small value of path loss exponent for Ground Floor is due to the NLOS nature of the data. For Car Park B3 small value of path loss exponent is due to the slope which creates a NLOS

scenario.

The path arrival time for the 1st path is almost the same for all the confined spaces. For Floor G and Floor 1 the other paths arrive at a larger time because of NLOS in Floor G and open space in Floor 1.

The channel statistics show that for Floor LA and Floor G we have a large excess delay and rms delay spread, resulting in a smaller coherence bandwidth. Whereas for the Floor 1 and B3 we have a smaller excess delay and higher coherence bandwidth.

Diffraction loss has also been computed theoretically for Floor 1 using the Knife edge geometry and practically taking the power difference. There is a difference of 6 dB in the results which is due to the approximation in the theoretical model.

ACKNOWLEDGEMENTS

This work was carried out under SABIC Fast track project SB-00910. The authors would like to thank King Fahd University of Petroleum and Minerals for this research opportunity.

REFERENCES

- A. Chandra, A. Kumar, P. (1999). Comparative study of path losses from propagation measurements at 450 mhz, 900 mhz, 1.35 ghz and 1.89 ghz in the corridors of a multifloor laboratory-cum-office building. In *IEEE Vehicular Technology Conference (VTC 1999-Fall)*, Amsterdam, the Netherlands.
- Abdellah Chehri, Paul Fortier, P. M. T. Characterization of the ultra-wideband channel in confined environments with diffracting rough surfaces. In *Wireless Pers Commun DOI 10.1007/s11277-010-0097-2*.
- Asrar Sheikh, Muhammad Imran Akram, M. K. (2010). Wireless channel characterization in an indoor environment. In *The 13th International Symposium on Wireless Personal Multimedia Communications (WPMC 2010)*.
- E., D. L. O. (Jan. 1952). Propagation studies at microwave frequencies by means of very short pulses. In *BSTJ*, pp. 91-103.
- Hawbaker, D. and T.S.Rappaport (1990). Indoor wideband radiowave propagation measurements at 1.3 ghz and 4.0 ghz. In *Electronics Letters*, Vol.26, No. 1.
- H.Hashemi (July 1993). The indoor radio propagation channel. In *Proceedings of the IEEE*, Vol.81 No.7 pp. 943- 968.
- J. Francois, M. L. (1990). Measurement and modeling of propagation losses in a building at 900 mhz. In *IEEE Transaction on vehicular technology*, Vol.39, No. 2.
- Poon, A. S. Y. and Ho, M. (2003). Indoor multiple-antenna channel characterization from 2 to 8 ghz. In *ICommunications and Interconnect Lab, Intel Corporation*.
- SALOUS, S. H. (1999). Wideband mobile radio channel characterization. In *Annals of Telecommunications, Volume 54, Numbers 1-2, 103-11*.
- Seidel, S. and Rappaport, T. (1992). 914 mhz path loss prediction models for wireless communications in multi-floored buildings. In *IEEE Trans. Antennas Propagation. Vol.40, No.2, pp.207-217*.
- Simon Chiu, J. C. and Michelson, D. G. (March 2010). Characterization of uwb channel impulse responses within the passenger cabin of a boeing 737-200 aircraft. In *IEEE Transactions on Antennas and Propagation page:935 vol:58 issue:3*.
- T.S.Rappaport (2002). *Wireless Communications: Principles and Practice*. Prentice Hall, 2nd edition.
- Turin G. L., Clapp E. D., J. T. L. F. S. B. L. D. (1972). A statistical model of urban multipath propagation. In *IEEE Trans. on VT, 21, pp. 1-9*.
- U. Dersch, J. T. and Zollinger, E. (1994). Multiple reflections of radio waves in a corridor. In *IEEE Trans. on Antenna and Propagation, Vol. 42, No.9, pp. 1571- 1574*.
- X. Zhao, J. Kivinen, P. V. K. S. (April 2002). Propagation characteristics for wideband outdoor mobile communications at 5.3 ghz. In *IEEE Journal on selected areas in communications, vol. 20, NO. 3*.
- Young W. R., L. L. Y. (March 1950). Echoes in transmission at 450 megacycles from land-to-car radio units. In *Proc. IRE, 38, pp. 255-258*.